

# ON INSTABILITIES OF CONVENTIONAL MULTI-COIL MRI RECONSTRUCTION TO SMALL ADVERSARIAL PERTURBATIONS

Chi Zhang<sup>1,2,\*</sup>, Jinghan Jia<sup>3,\*</sup>, Burhaneddin Yaman<sup>1,2,\*</sup>, Steen Moeller<sup>2</sup>, Sijia Liu<sup>4</sup>, Mingyi Hong<sup>1</sup>, and Mehmet Akçakaya<sup>1,2</sup>  
<sup>1</sup>Electrical and Computer Engineering, and <sup>2</sup>Center for Magnetic Resonance Research, University of Minnesota, Minneapolis, MN, United States

<sup>3</sup>University of Florida, Gainesville, FL, United States

<sup>4</sup>MIT-IBM Watson AI Lab, IBM Research, Cambridge, MA, United States

**SYNOPSIS:** Although deep learning (DL) has received much attention in accelerated MRI, recent studies suggest small perturbations may lead to instabilities in DL-based reconstructions, leading to concern for their clinical application. However, these works focus on single-coil acquisitions, which is not practical. We investigate instabilities caused by small adversarial attacks for multi-coil acquisitions. Our results suggest that, parallel imaging and multi-coil CS exhibit considerable instabilities against small adversarial perturbations.

**KEY FINDINGS:** Conventional multi-coil reconstructions are also susceptible to large instabilities from small adversarial perturbations. It is worthwhile to interpret the instabilities of DL methods within this broader context for the practical multi-coil setting.

**INTRODUCTION:** Deep learning (DL) reconstruction has recently received much attention due to its improved reconstruction quality<sup>1-5</sup>. While DL has been transformative in many image processing tasks, it is well-understood that these methods may be susceptible to instabilities arising from small adversarial perturbations due to their non-linear nature<sup>6-8</sup>. Such instabilities were also explored for MRI reconstruction recently<sup>9</sup>, which suggested that both researchers and FDA need to be cognizant of these issues. Several follow-up studies<sup>10,11</sup> explored adversarial training frameworks to improve the robustness of DL-MRI reconstruction. However, all these works concentrated on a single-coil setup, which has little practical application.

In this work, we investigate how small adversarial perturbations affect multi-coil MRI reconstruction, particularly using conventional non-DL methods. Our results indicate that for multi-coil MRI reconstruction, parallel imaging and multi-coil compressed sensing (CS) methods are also susceptible to large instabilities from small adversarial perturbations.

## METHODS:

Multi-coil MRI Acquisition Model and Inverse Problem: The multi-coil encoding model is given as

$$\mathbf{y}_\Omega = \mathbf{E}_\Omega \mathbf{x} + \mathbf{n}, \quad (1)$$

where  $\mathbf{y}_\Omega$  is the acquired measurements with sub-sampling pattern  $\Omega$ ,  $\mathbf{E}_\Omega$  is the multi-coil encoding matrix, and  $\mathbf{n}$  is noise. For i.i.d. Gaussian noise, the maximum likelihood estimate is

$$\arg \min_{\mathbf{x}} \|\mathbf{y}_\Omega - \mathbf{E}_\Omega \mathbf{x}\|_2^2 = (\mathbf{E}_\Omega^H \mathbf{E}_\Omega)^{-1} \mathbf{E}_\Omega^H \mathbf{y}_\Omega, \quad (2)$$

which is the CG-SENSE<sup>12</sup> output without regularization. Alternatively, a regularized version of the problem can be solved

$$\arg \min_{\mathbf{x}} \|\mathbf{y}_\Omega - \mathbf{E}_\Omega \mathbf{x}\|_2^2 + \mathcal{R}(\mathbf{x}) \quad (3)$$

where  $\mathcal{R}(\cdot)$  is a regularizer, e.g. Tikhonov or  $l_1$ -norm of transform coefficients. In DL methods that rely on algorithm unrolling<sup>5</sup>, the regularizer is implicitly learned through neural networks, leading to a non-linear representation.

Adversarial Attacks: Let  $\mathbf{z}_\Omega = \mathbf{E}_\Omega^H \mathbf{y}_\Omega$  denote the zero-filled image, and  $f(\mathbf{z}_\Omega)$  be a reconstruction algorithm that takes as input the zero-filled image. Note that while the reconstruction algorithm may take  $\mathbf{y}_\Omega$  as input, using the zero-filled image allows consistency with the setup in<sup>9</sup>. We use an  $l_\infty$ -attack, i.e. the attack  $\mathbf{r}$  on the input with  $\|\mathbf{r}\|_\infty < \epsilon$  leads to a reconstruction  $f(\mathbf{z}_\Omega + \mathbf{r})$  that largely deviates from the original output  $f(\mathbf{z}_\Omega)$ . The attack is chosen on the zero-filled image instead of the fully-sampled image as done in<sup>9</sup>, because the latter is not practical: 1) One does not have access to fully-sampled images to generate a practical attack, 2) In multi-coil MRI, the encoding operator is not known exactly, but estimated. Finally, the attack is not chosen in k-space, since it is difficult to define an  $l_\infty$ -perturbation in k-space due to the varying signal strength between center and edges.

Imaging Data and Experiments: Coronal proton density knee MRI with 15-channel coils were obtained from the fastMRI database<sup>13</sup>. An acceleration rate,  $R = 4$  with 24 ACS lines was used, as common in DL-MRI reconstruction<sup>14</sup>.

Both uniform and random undersampling were investigated. For the former, CG-SENSE and GRAPPA were considered, while for the latter, CG-SENSE and multi-coil CS were explored. For both undersampling patterns, the attacks were performed on the CG-SENSE solution. Specifically, the CG algorithm was unrolled for 10 iterations<sup>3</sup>. The attack was generated on this unrolled CG using fast gradient sign method<sup>15</sup> with an MSE loss and  $\epsilon = \|\mathbf{z}_\Omega\|_\infty / 255$  (Fig. 1). For random undersampling, this attack was used directly on multi-coil CS. For uniform undersampling, the small perturbation attack on the zero-filled image was converted to k-space for GRAPPA. Among the infinitely many k-space perturbations on  $\Omega$  that led to  $\mathbf{r}$ , the minimum  $l_2$  solution was picked.

For testing, CG-SENSE used 10 iterations; GRAPPA used  $5 \times 4$  kernels. Multi-coil CS reconstruction utilized variable splitting,  $l_1$ -norm of Daubechies4 wavelets as the regularizer, and its parameters were tuned empirically. All coil maps were generated using ESPIRiT<sup>16</sup>.

Additionally, an attack was generated on a pre-trained DL method<sup>17,18</sup> based on an unrolled network to investigate whether the linear data-consistency units or the non-linear neural networks used for regularization were affected more substantially.

### **RESULTS:**

Fig. 2 depicts CG-SENSE and GRAPPA results for uniform undersampling. While the perturbation causes no visual difference in the fully-sampled image, both methods fail under the attack. Fig. 3 shows CG-SENSE and multi-coil CS reconstructions for random undersampling. The same conclusions apply, with both methods failing under a non-visible small perturbation.

Fig. 4 depicts the results of an unrolled neural network under an attack that targets it end-to-end. There is no major change when the attack is run through a single regularizer unit, but output collapses when the attack is passed through a single data-consistency unit. This suggests the end-to-end attack on an unrolled network targets the linear data-consistency units.

### **DISCUSSION AND CONCLUSIONS:**

Our results indicate that for multi-coil MRI reconstruction, parallel imaging and multi-coil CS are also susceptible to large instabilities from small adversarial perturbations. Moreover, for DL reconstruction that utilize  $\mathbf{E}_\Omega$  explicitly, adversarial attacks predominantly target the linear data-consistency units. The ill-conditioning of the encoding operator is well-discussed for CG-SENSE in non-Cartesian acquisitions, which has led to an early stopping criterion in practice<sup>19</sup>. While in general, it is hard to compute the condition number, which depends on the coil configuration and  $\mathbf{R}$ , adversarial attacks enable a method to exploit such ill-conditioning. Since these attacks also breakdown multi-coil MRI reconstruction methods, including parallel imaging and CS, it is worthwhile to interpret the instabilities of DL methods within this broader context.

**ACKNOWLEDGEMENTS:** \*The first three authors contributed equally to this work. Grant support: NIH R01HL153146, NIH P41EB027061, NIH U01EB025144; NSF CAREER CCF-1651825

### **References**

1. Wang S, Su Z, Ying L, et al. Accelerating magnetic resonance imaging via deep learning. IEEE 13th International Symposium on Biomedical Imaging (ISBI); 2016; 514-517.
2. Hammernik K, Klatzer T, Kobler E, et al. Learning a variational network for reconstruction of accelerated MRI data. Magn Reson Med. 2018; 79(6):3055-3071.
3. Aggarwal HK, Mani MP, Jacob M. MoDL: Model-Based Deep Learning Architecture for Inverse Problems. IEEE Trans Med Imaging. 2019; 38(2):394-405.
4. Schlemper J, Caballero J, Hajnal JV, et al. A Deep Cascade of Convolutional Neural Networks for Dynamic MR Image Reconstruction. IEEE Transactions on Medical Imaging. 2018; 37(2): 491-503. doi:10.1109/tmi.2017.2760978
5. Knoll F, Hammernik K, Zhang C, et al. Deep Learning Methods for Parallel Magnetic Resonance Image Reconstruction. IEEE Signal Processing Magazine. 2020; 37(1):128-140.
6. Moosavi-Dezfooli SM, Fawzi A, Frossard P. Deepfool: A simple and accurate method to fool deep neural networks. Proc. IEEE Conference on Computer Vision and Pattern Recognition. 2016; 2574-2582.
7. Moosavi-Dezfooli SM, Fawzi A, Fawzi O, et al. Universal adversarial perturbations. Proc. IEEE Conference on Computer Vision and Pattern Recognition. 2017; 86-94.

8. Szegedy C, Zaremba W, Sutskever I, et al. Intriguing properties of neural networks. Proc. International Conference on Learning Representations. [https://openreview.net/forum?id=kklr\\_MTHMRQjG](https://openreview.net/forum?id=kklr_MTHMRQjG). Accessed 28 April 2020.
9. Antun V, Renna F, Poon C. On instabilities of deep learning in image reconstruction and the potential costs of AI. Proc. PNAS. 2020; 117(48):30088–30095.
10. Raj A, Bresler Y, Li B. Improving Robustness of Deep-Learning-Based Image Reconstruction. arXiv preprint. 2020; arXiv:2002.11821.
11. Genzel M, Macdonald J, März M. Solving Inverse Problems With Deep Neural Networks--Robustness Included? arXiv preprint. 2020; arXiv:2011.04268.
12. Pruessmann KP, Weiger M, Börnert P, et al. Advances in Sensitivity Encoding With Arbitrary k-Space Trajectories, Magn Reson Med. 46:638–651.
13. Knoll F, Zbontar J, Sriram A, et al. fastMRI: A Publicly Available Raw k-Space and DICOM Dataset of Knee Images for Accelerated MR Image Reconstruction Using Machine Learning. Radiology: Artificial Intelligence. 2020; 2(1): e190007.
14. Knoll F, Murrell T, Sriram A, et al. Advancing machine learning for MR image reconstruction with an open competition: Overview of the 2019 fastMRI challenge. Magn Reson Med. 2020; 84:3054–3070.
15. Goodfellow IJ, Shlens J, Szegedy C. Explaining and Harnessing Adversarial Examples. arXiv preprint. 2014; arXiv:1412.6572.
16. Uecker M, Lai P, Murphy M J, et al. ESPIRiT—an eigenvalue approach to autocalibrating parallel MRI: where SENSE meets GRAPPA. Magn Reson Med. 2014; 71(3):990-1001.
17. Yaman B, Hosseini SAH, Moeller S, et al. Self-supervised learning of physics-guided reconstruction neural networks without fully sampled reference data. Magn Reson Med. 2020; 84:3172–3191.
18. Hosseini SAH, Yaman B, Moeller S, et al. Dense recurrent neural networks for accelerated MRI: History-cognizant unrolling of optimization algorithms. IEEE J Selec Top Sign Proc. 2020; 14(6):1280-1291.
19. Maier O, Baete SH, Fyrdahl A, et al. CG-SENSE revisited: Results from the first ISMRM reproducibility challenge. arXiv preprint. 2020; arXiv:2008.04308.

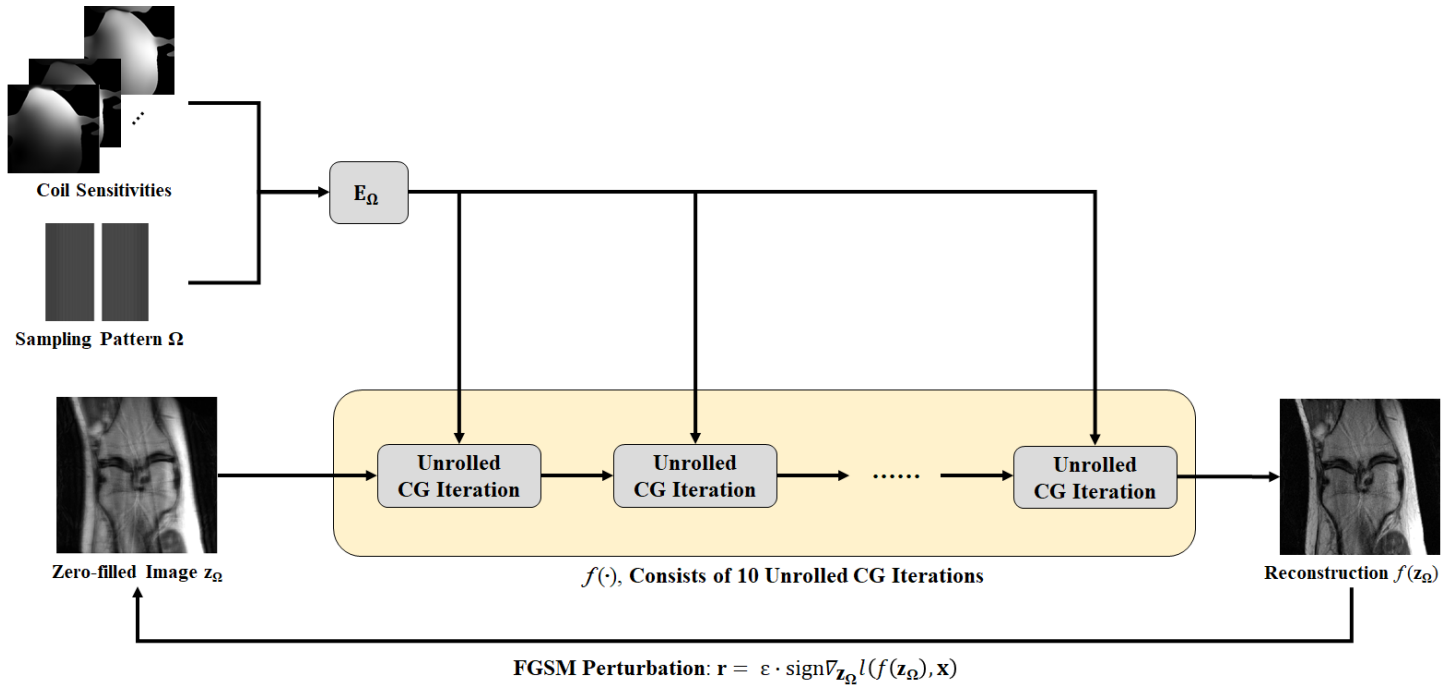


**Figure 1.** The process for generating the small adversarial perturbation using unrolled CG-SENSE. Fast gradient sign method (FGSM) is used to generate the perturbation  $\mathbf{r}$  via a single backpropagation through the unrolled CG algorithm, where  $l(\cdot, \cdot)$  denotes MSE loss. For testing,  $\mathbf{r}$  is added to the zero-filled image,  $\mathbf{z}_\Omega$ , which is then run through the relevant reconstruction algorithm.

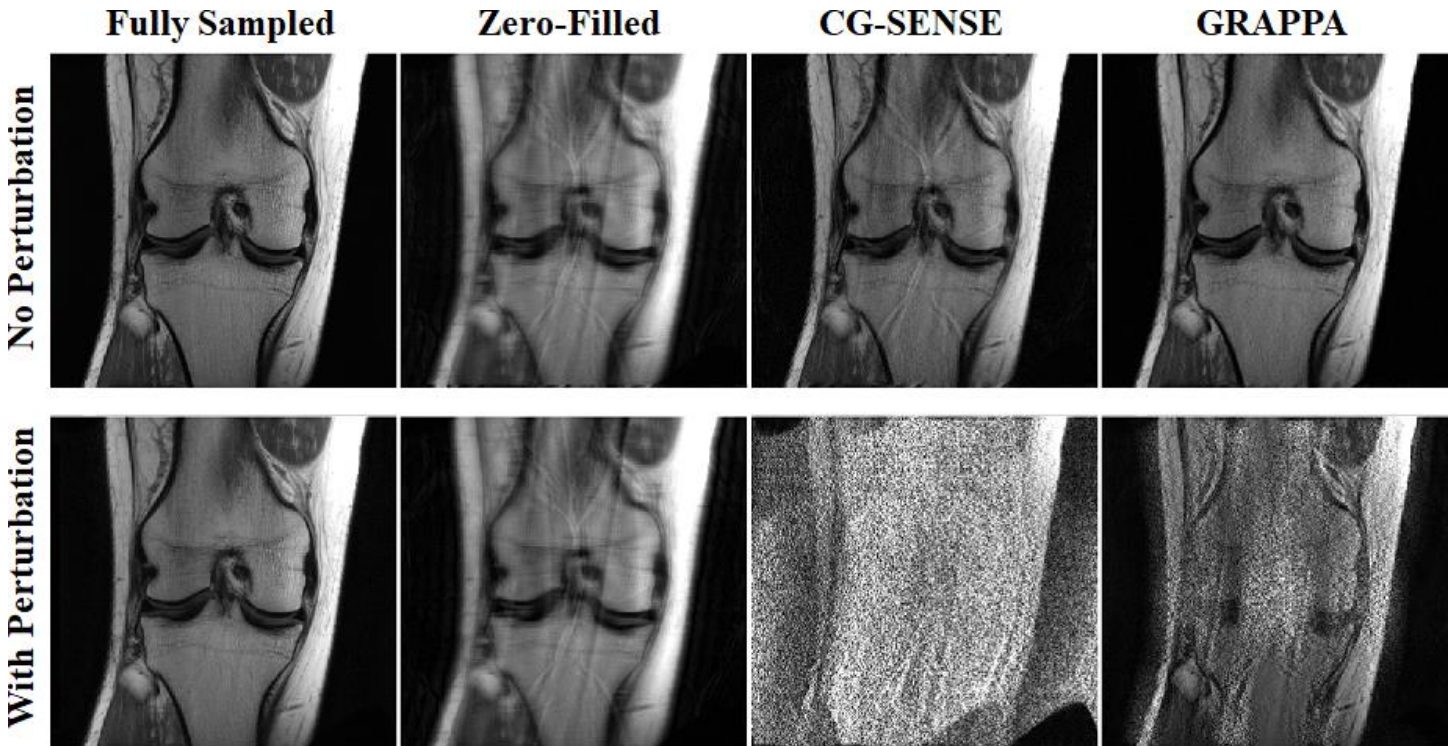


**Figure 2.** Reconstruction results for uniform undersampling without (top row) and with (bottom row) attack. The small perturbation causes no visual difference in the fully-sampled image or the zero-filled image. The reconstructions without attack show some residual aliasing due to the R=4 acceleration. Both CG-SENSE and GRAPPA visibly fail with the small perturbation attack.

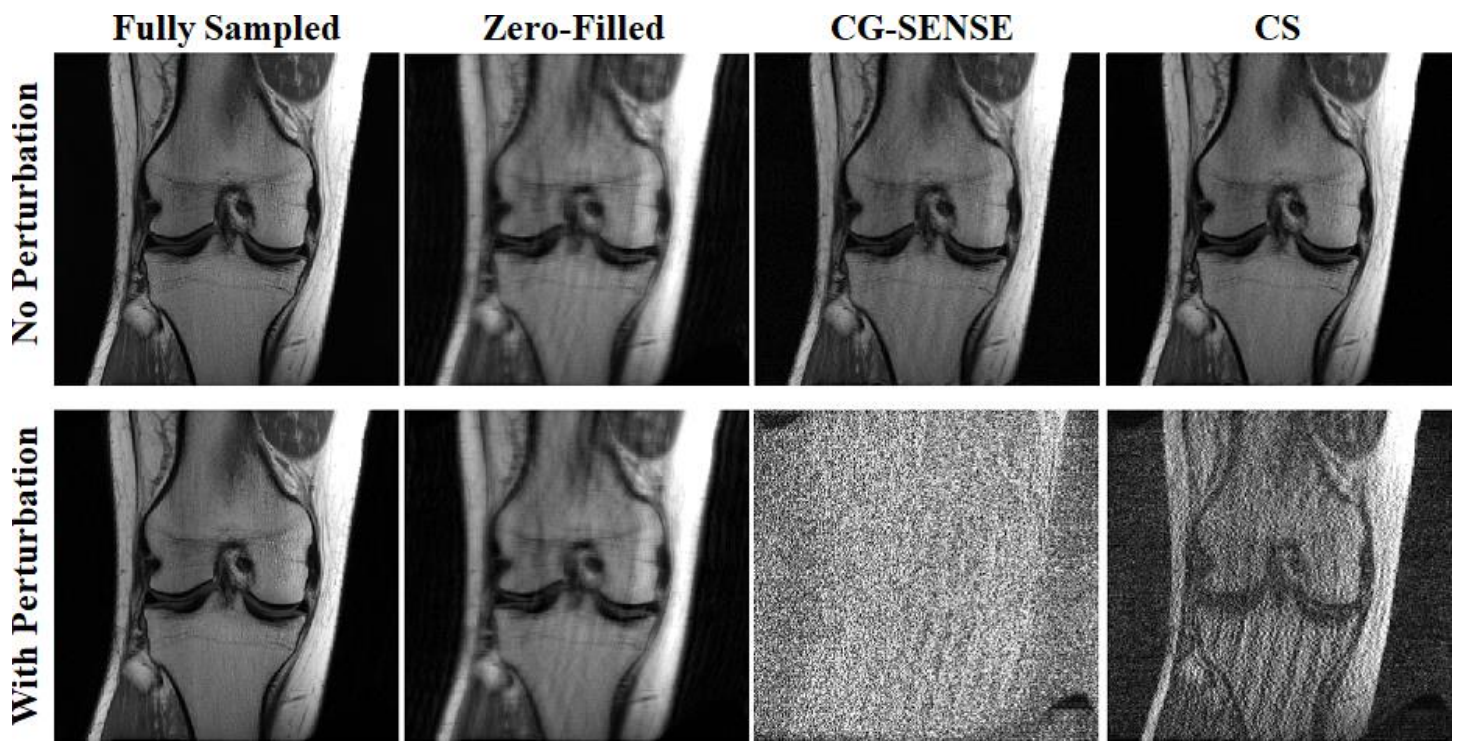
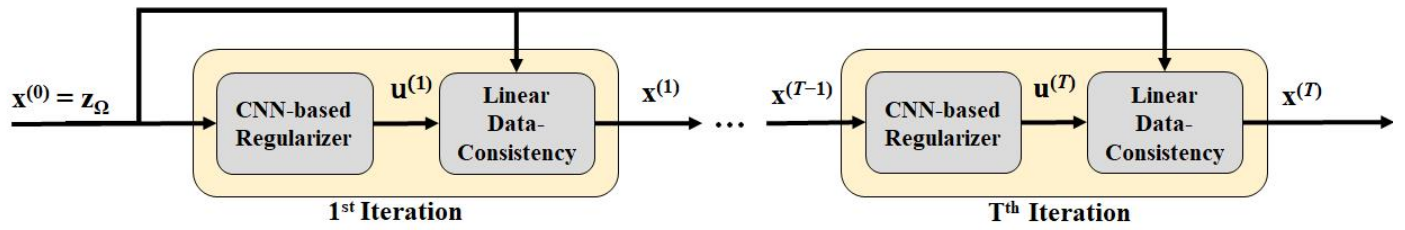


**Figure 3.** Reconstruction results for random undersampling without (top row) and with (bottom row) attack. The small perturbation leads to no visual change in the fully-sampled or zero-filled image. For the input without attack, CG-SENSE has visible and multi-coil CS has subtle aliasing artifacts at  $R=4$ . For the attack input, both these reconstructions fail although they are run with the exact same parameters as the non-attack case.

(a)



$$\text{Regularizer CNN: } \mathbf{u}^{(i)} = \arg \min_{\mathbf{u}} \mu \|\mathbf{x}^{(i-1)} - \mathbf{u}\|_2^2 + \mathcal{R}(\mathbf{u})$$

$$\text{Linear Data-Consistency: } \mathbf{x}^{(i)} = (\mathbf{E}_\Omega^H \mathbf{E}_\Omega + \mu \mathbf{I})^{-1} (\mathbf{z}_\Omega + \mu \mathbf{u}^{(i)})$$

(b)

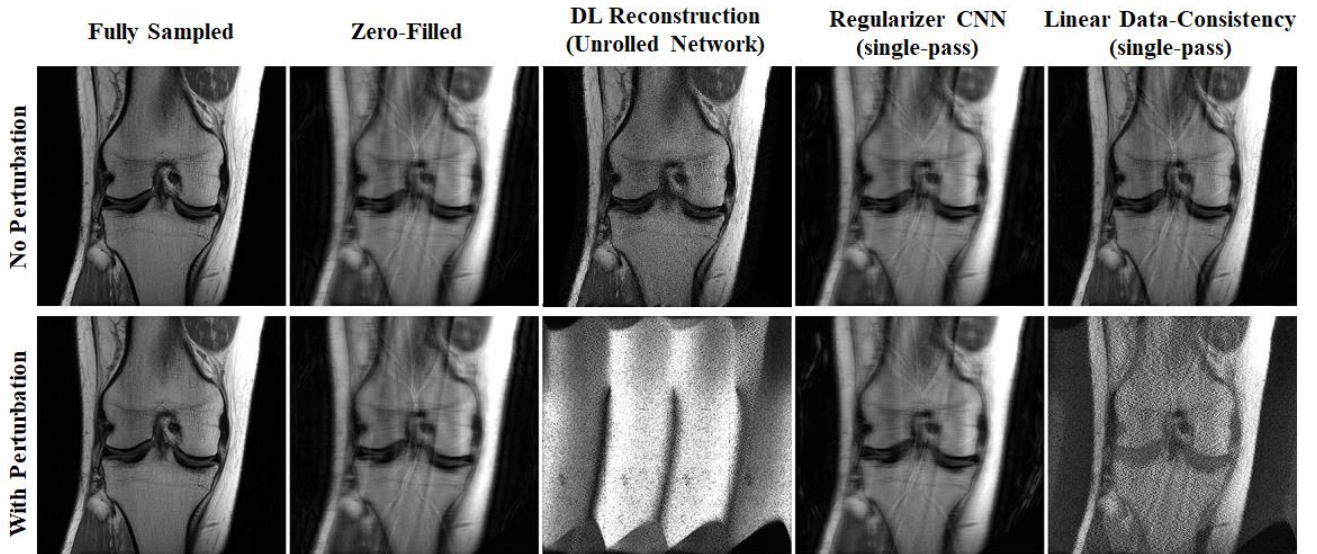


**Figure 4.** (a) Schematic of the unrolled network, with ResNet regularizer and linear data-consistency (DC) unit. (b) DL results for uniform undersampling. Perturbation does not visually alter fully-sampled or zero-filled images. Without attack, DL leads to good quality. With the attack, DL collapses, as with conventional methods in Fig. 2&3. The attack through a single CNN regularizer (4th col.) shows no alteration, but it shows visible degradation through a single data-consistency (5th col.), suggesting the attack targets linear DC units more than CNN regularizers in the unrolled network.